On-chip all-optical multicasting of mode-division multiplexing QPSK signals

Baobao Chen[1, 2], Yi Zhao[1, 2], Haoyang Tan[1, 2], Xiaowei Guan[3, 4] and Shiming Gao[1, 2]

[1] *Center for Optical and Electromagnetic Research, State Key Laboratory of Modern Optical Instrumentation, International Research Center for Advanced Photonics, Zhejiang University, Hangzhou, China*
[2] *Ningbo Research Institute, Zhejiang University, Ningbo, China*
[3] *Intelligent Optics & Photonics Research Center, Jiaxing Institute of Zhejiang University, Jiaxing, China*
[4] *Department of Photonics Engineering, Technical University of Denmark, Ørsteds Plads, Building 345A, 2800 Kgs. Lyngby, Denmark*

Email: gaosm@zju.edu.cn

We propose and experimentally demonstrate an on-chip all-optical multicasting (AOM) for 40 Gbit/s mode-division-multiplexed quadrature phase-shift keying (MDM-QPSK) signals based on a parallel dispersion-engineered multimode nonlinear silicon waveguide. Five dual-mode multicast wavelengths are successfully obtained on the generate idlers, and the power penalties of all the multicast channels are less than 1.1 dB at the bit error rate (BER) of 3.8×10^{-3}. The dual-mode AOM scheme has the potential to promote the ability of optical cross-connect in practical hybrid multiplexed networks including MDM channels.

Introduction: All-optical multicasting (AOM), a kind of significant wavelength-routed network technologies, simultaneously copies the same data on the incoming signal wavelength to multiple different outgoing wavelengths for multiple different destinations [1]. AOM has the ability to support optical cross-connect (OXC) at nodes to increase the configurability in future optical networks [2], which supports OXC to realize more functions, such as broadcast, select, route, partial multicast, and multicast [3]. AOM can be realized based on light splitting [4] or multiple four-wave mixing (FWM) effect [5, 6]. In the former scheme, the multicasting copies are obtained by splitting the signal using optical splitters, and thus it has to suffer from a high loss. While in the latter scheme, the different wavelength copies are generated by the incoming signal through multiple FWM processes assisted by several pumps [7]. Thanks to the excellent performance of FWM, this kind of AOM exhibits strict transparency to modulation format and bit rate.

To satisfy the speedy growth bandwidth demand, multiplexing technologies have been well developed, such as wavelength-division multiplexing (WDM), mode-division multiplexing (MDM), and polarization-division multiplexing (PDM), which can transmit multi-channel signals in parallel [8]. Besides these multiplexing technologies, advanced modulation formats are also well used to extremely increase the spectral efficiency [9]. In this case, the demonstration of AOM for multiplexing signals with advanced modulation formats becomes urgent. For PDM signals, the AOM function can be achieved using a polarization-angled pump to support the FWM processes on the two orthogonal polarization states simultaneously [10]. While for MDM signals, it is challengeable to simultaneously engineer the dispersion profiles for different modes so as to satisfy all the phase-matching conditions. In the past, on-chip mode-selective wavelength conversion for MDM signals have been carried out, just to satisfy the phase-matching condition for a single mode [11]. Moreover, we have demonstrated the wavelength conversion for MDM signal by carefully design the silicon waveguide

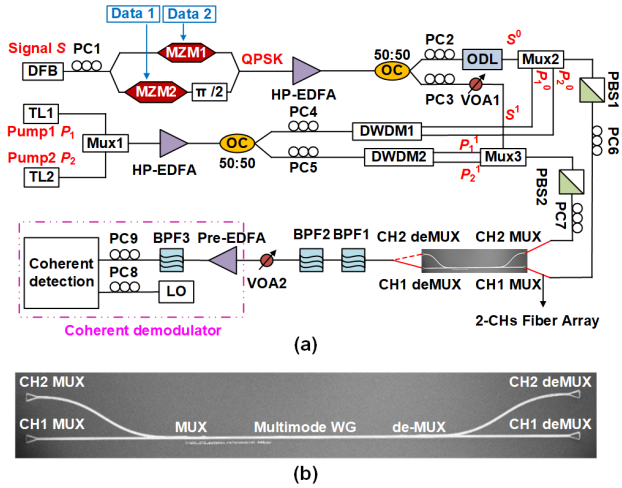

Fig 1 *(a) Experiment setup of the AOM for dual-mode QPSK signals in a silicon waveguide. (b) Silicon waveguide structure.*

structure to support multiple FWM processes simultaneously [12], as well as realized the wavelength conversion for hybrid WDM-MDM signals [13]. However, AOM for MDM signals has not been reported so far.

In this letter, we propose and experimentally demonstrate a dual-mode AOM for 40 Gbit/s MDM-QPSK signals in a parallel dispersion-engineered multimode nonlinear silicon waveguide with dual-wavelength pumps. An input MDM signal is simultaneously replicated to multiple wavelengths carrying the same MDM data. Five multicast wavelengths are obtained and the power penalties of the MDM wavelength multicasting are all less than 1.1 dB when the BER is 3.8×10^{-3} (the forward error correction threshold).

Experimental scheme: Fig. 1(a) depicts the experimental setup for the proposed AOM in a multimode silicon waveguide driven by dual-pump for dual-mode QPSK signals. The waveguide is with a height of 220 nm and a width of 770 nm, which is dispersion-engineered for TE_0 and TE_1 modes to realize their zero-dispersion wavelengths are both near 1550 nm. The conversion bandwidths of waveguide are measured to be about 68 nm for the two modes [13]. The nonlinear coefficients of the two modes at 1550 nm are calculate to be 139.2 $W^{-1}m^{-1}$ and 134 $W^{-1}m^{-1}$, respectively. The waveguide structure is shown in Fig. 1(b). In our experiment, the optical carrier is served by a distributed feedback laser (DFB) with a wavelength of 1549.3 nm. The QPSK signal is generated by modulating two 10 Gbit/s 2^{15}-1 NRZ pseudo-random binary sequences (PRBSs) through the integrated in-phase quadrature (IQ) optical transmitter module, which consists of a lithium niobate-based electro-optical I/Q modulator (Fujitsu FTM7961EX), an automatic bias controller and a RF driver. After being amplified by a HP-EDFA, the QPSK signal is split into two tributaries through a 50:50 optical couplers (OC) and de-correlated using an optical delay line (ODL). Due to the different nonlinear coefficients between TE_0 and TE_1 modes, the conversion efficiencies (CEs) are different for two modes if their input powers are the same. Here, a variable optical attenuator (VOA) is introduced in another tributary to change the power and ensure the CEs of two modes almost the same. The two pumps are provided by a multi-channel tunable laser (TL) (Agilent N7714A) and combined by Mux1. Thereafter, the two pumps are amplified and split into two paths, combining with the two tributaries of input signal respectively. The polarization beam splitter (PBS) are utilized to keep the polarization states of the signal and pumps co-polarized. To ensure the maximum powers of co-

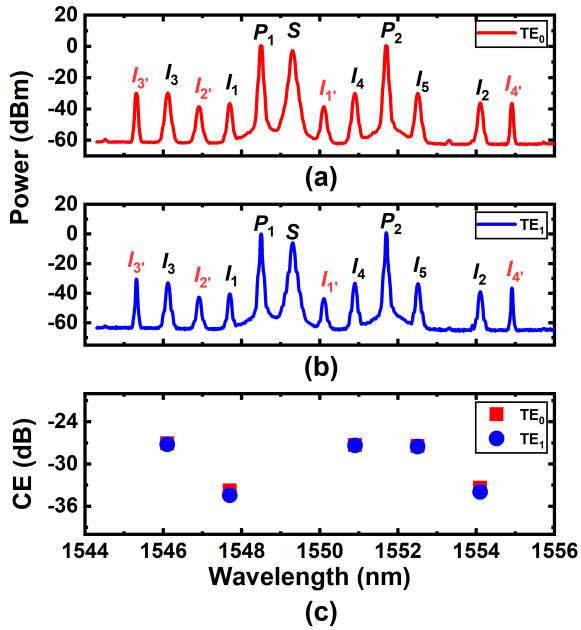

Fig 2 *Measured optical spectrums of the AOM for MDM-QPSK signals at the output ports CH1 (a) and CH2 (b) of the silicon waveguide. (c) CEs versus various multicast wavelength channels.*

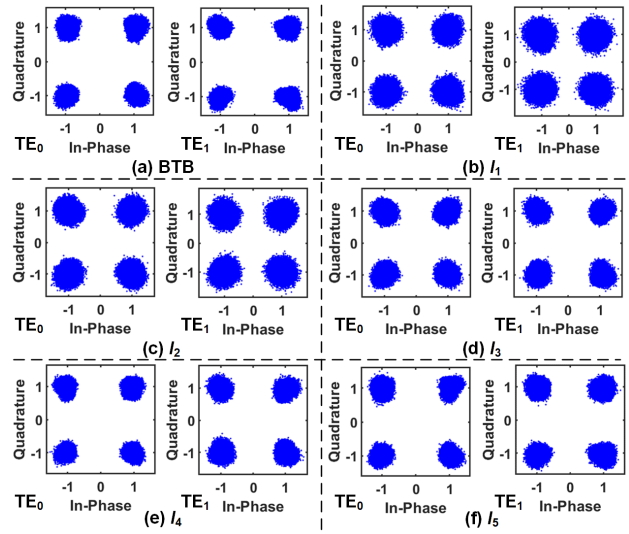

Fig 3 *Constellation diagrams of (a) back to back (BTB) of the input signal at 1549.3 nm and the dual-mode multicasting idlers (b) I_1 at 1547.7 nm, (c) I_2 at 1545.1 nm, (d) I_3 at 1546.1 nm, (e) I_4 at 1550.7 nm, and (f) I_5 at 1552.5 nm.*

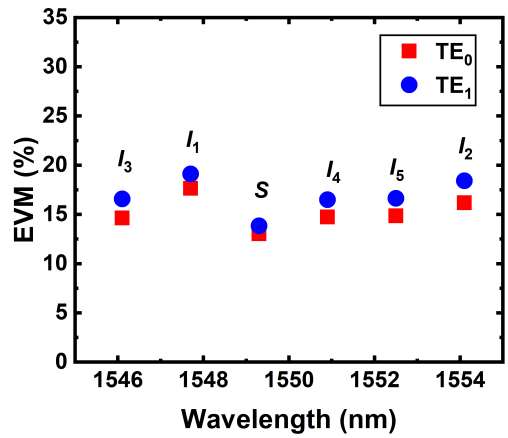

Fig. 4 *EVMs versus various multicast wavelength channels.*

polarized signal and pumps, PC2-PC5 are introduced to adjust their polarizations. By adjusting PC6 and PC7, the polarization states of the signal and pumps are aligned with the TE axis of the silicon waveguide to achieve the maximum CEs. Two paths that both consist of QPSK signal and dual pumps are coupled into the waveguide simultaneously via a two-channel optical fiber array (OFA) with a 127-μm pitch. The path of CH1 MUX port is coupled into the nonlinear waveguide as TE_0 mode, while the path from CH2 MUX port is converted to TE_1 mode through a mode multiplexer. In the waveguide, a series of FWM processes occur among the incident MDM-QPSK signal S and the dual pumps P_1 and P_2, including inter-mode and intra-mode processes in principle. However, the inter-mode FWMs can be neglected due to their large phase mismatches [13]. The intra-mode FWMs can be divided into two series: degenerate FWMs ($2P_1 \rightarrow S + I_1$ and $2P_2 \rightarrow S + I_2$) and non-degenerate FWMs ($P_1 + S \rightarrow P_2 + I_3$, $P_1 + P_2 \rightarrow S + I_4$ and $P_2 + S \rightarrow P_1 + I_5$). Via these intra-mode FWMs, five-wavelength idlers with dual-mode channels are generated at the output ports of the silicon waveguide, which carry the same 40 Gbit/s MDM-QPSK data as that on the input signal. The TE_0 signals are output from CH1 deMUX port, while the TE_1 mode signals are converted back to TE_0 mode through a mode de-multiplexer and output at CH2 deMUX port. The 0.8-nm band pass filters (BPF) are used to select the generated idlers. For the performance measurement of the dual-mode AOM, a VOA is used to change the received power of the QPSK signal. Each multicasting channel can be demodulated by a coherent demodulator, which consists of a pre-amplifier (Pre-EDFA), a BPF, a local oscillator (LO) (Agilent 81940), and a coherent receiver (u^2t photonics CPRV1220A). The signal is sampled at 25 GSa/s via a 20 GHz bandwidth real-time digital oscilloscope (Tektronix MSO72004C).

Results and discussion: Fig. 2 shows the measured optical spectrums of the AOM for dual-mode (TE_0 mode in Fig. 2(a) and TE_1 mode in Fig. 2(b)) QPSK signals at the output ports of the waveguide via an optical spectrum analyzer (AQ6370C) with the resolution of 0.05 nm. The two pumps (P_1 and P_2) are set at 1548.5 nm and 1551.7 nm and the powers in each tributary before the silicon waveguide are 24.1 dBm and 23.7 dBm, respectively. The signal power of each tributary is 20.2 dBm. The total losses are 15.1 dB, which can be attributed to the fiber-grating coupling loss of approximate 7.3 dB/facet. Nine idlers can be observed in Fig. 2, including five multicasting idlers reserving the signal information, two idlers (1546.9 nm and 1550.1 nm) generated by FWM processes ($2S \rightarrow P_2 + I_{2'}$ and $2S \rightarrow P_1 + I_{1'}$), which phase information differ from the input signal, and two idlers (1545.3 nm and 1554.9 nm) generated by the FWM processes only between pumps ($2P_1 \rightarrow P_2 + I_{4'}$ and $2P_2 \rightarrow P_1 + I_{3'}$). The five multicasting wavelengths are I_1 (1547.7 nm), I_2 (1554.1 nm), I_3 (1546.1 nm), I_4 (1550.9 nm), and I_5 (1552.5 nm), whose CEs are calculated from the spectrums, as shown in Fig. 2(c). The CEs are -33.8, -33.4, -27.1, -27.3, and -27.4 dB for TE_0 mode, and -34.4, -33.9, -27.2, -27.4, and -27.5 dB for TE_1 mode, respectively. In Fig. 2(c), the CEs of the two modes have excellent equalization, and the CEs of degenerate FWM processes (I_1 and I_2) are a little lower than that of the non-degenerate FWMs (I_3, I_4 and I_5).

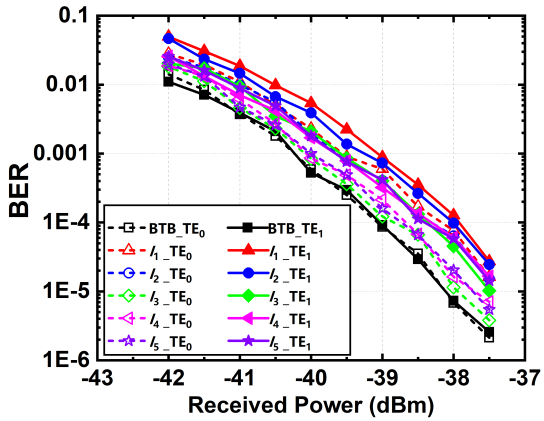

Fig 5 *Measured BER performance against the received power for the BTB signal and the AOM idlers with TE_0 and TE_1 mode.*

Fig. 3 shows the constellation diagrams of the original MDM-QPSK signal and the five multicasting wavelengths through digital coherent detection. The back-to-back (BTB) constellation diagrams measured before the silicon waveguide are shown in Fig. 3(a), and the multicasting constellation diagrams are shown in Fig. 3(b)-(f). To evaluated the multicasting quality quantitatively, the root-mean-square (RMS) error vector magnitudes (EVMs) are calculated, as shown in Fig. 4. The BTB RMS EVMs are 13.04% and 13.85% for TE_0 and TE_1 modes, respectively. That of the idlers, which fluctuates from 14.63% to 19.11%, shows a little degradation. Comparing the EVMs of the two modes, one can find that they are quite similar (their maximum RMS EVMs difference is less than 2.24%), and TE_0 mode is a little better than TE_1 mode.

Fig. 5 shows the measured BER results of the five dual-mode multicasting idlers as a function of the received power compared with the BTB signal. In the BTB case, the required received powers for the two modes are both -40.8 dBm at the BER of 3.8×10^{-3}. For the dual-mode multicasting idlers generated by non-degenerate FWM processes, the power penalties are less than 0.3 dB for TE_0 mode and 0.6 dB for TE_1 mode, while they are less than 0.7 dB and 1.1 dB for degenerate FWM multicasting idlers. The BER performances of idlers from non-degenerates FWM are a little better than that from degenerate FWM, which agrees well with the analysis of constellation diagrams and CEs.

Conclusion: The multiple intra-mode FWM based AOM scheme has been proposed and experimentally demonstrated for MDM-QPSK signals in a parallel dispersion-engineered multimode nonlinear silicon waveguide. By using two dual-mode pumps, five dual-mode multicasting wavelengths are generated with the efficiencies of above -34.4 dB. Also, the RMS EVMs of the multicasting constellation diagrams are less than 19.1%. Moreover, the dual-mode idlers show excellent equalization. At BER of 3.8×10^{-3}, all five dual-mode multicast wavelengths show high qualities with a maximum power penalty of less than 1.1 dB for the TE_0 and TE_1 modes. If more pumps are utilized, more multicasting wavelength can be expected since the multimode nonlinear waveguide we used is broadband. The proposed scheme is promising to extend the functions of OXC in future high-capacity wavelength-routed networks.

Acknowledgments: This work was supported by the National Natural Science Foundation of China (U2141231) and the Zhejiang Provincial Natural Science Foundation of China (LDT23F04015F05).

Received: xx January 2021 *Accepted:* xx March 2021
doi: 10.1049/ell2.10001

References

1. Yang Y., et al.: Nonblocking WDM multicast switching networks. *IEEE Trans. Parallel Distrib. Syst.* **11**(12), 1274-1287 (2000)
2. Sahasrabuddhe L. H., Mukherjee B.: Light trees: optical multicasting for improved performance in wavelength routed networks. *IEEE Commun. Mag.* **37**(2), 67-73 (1999)
3. Wang D., et al.: Flexible optical cross-connect structures supporting WDM multicast with multiple pumps for multiple channels. *IEEE Photon. J.* **6**(6), 1-12, (2014)
4. Zhang X., et al.: Constrained multicast routing in WDM networks with sparse light splitting. *J. Lightw. Technol.* **18**(12), 1917-1927 (2000)
5. Wang D., et al.: Optical Network Node Supporting One-to-Six WDM Multicasting of QPSK Signals. *IEEE Photon. Technol. Lett.* **26**(16), 1641-1644 (2014)
6. Qin J., et al.: On-Chip High-Efficiency Channel-Selective Wavelength Multicasting of PAM3/PAM4 Signals using an AlGaAsOI Waveguide. *Conference on Lasers and Electro-Optics*, pp. 1-2, San Jose, CA (2020)
7. Gao X., et al.: Seven-channel all-optical reconfigurable canonical logic units multicasting at 40 Gb/s based on a nonlinearity-enhanced silicon waveguide. *Opt. Express* **30**(18), 32650-32659 (2022)
8. He Y., et al.: Design and experimental demonstration of a silicon multi-dimensional (de)multiplexer for wavelength-, mode- and polarization-division (de)multiplexing. *Opt. Lett.* **45**(10), 2846-2849 (2020)
9. Zou K., et al.: Demonstration of Free-Space 300-Gbit/s QPSK Communications Using Both Wavelength- and Mode- Division-Multiplexing in the Mid-IR. *Optical Fiber Communications Conference and Exhibition*, pp. 1-3, San Francisco, CA (2021).
10. Feng X., et all.: Integrated all-optical wavelength multicasting for 40 Gbit/s PDM-QPSK signals using a single silicon waveguide. *Opt. Laser Technol.* **94**, 261–266 (2017)
11. Qiu Y., et al.: Mode-selective wavelength conversion of OFDM-QPSK signals in a multimode silicon waveguide. *Opt. Express* **25**(4), 4493-4499 (2017)
12. Chen B., et al.: Silicon-based on-chip all-optical wavelength conversion for two-dimensional hybrid multiplexing signals. *J. Nonlinear Opt. Phys. Mater.* **28**(4), (2019)
13. Chen B., et al.: Broadband Wavelength Conversion for Hybrid Multiplexing Signals Based on a Parallel Dispersion-Engineered Silicon Waveguide. *IEEE Photon. J.* **15**(1), 1-7 (2023)